Desalination and Water Treatment
www.deswater.com

doi: 10.1080/19443994.2015.1063012

57 (2016) 14093–14108
June

Taylor & Francis
Taylor & Francis Group

Adsorption of anionic dyes from an aqueous solution by banana peel and green coconut mesocarp

Graziele Elisandra do Nascimento, Natália Ferreira Campos, Jailson José da Silva, Celmy Maria Bezerra de Menezes Barbosa, Marta Maria Menezes Bezerra Duarte*

Chemical Engineering Department, Federal University of Pernambuco, Avenida Artur de Sá, s/n, Recife 50740-521, Brazil, Tel. +558121267291; emails: grazielen@yahoo.com.br (G.E. do Nascimento), nataliaferreiracamp@hotmail.com (N.F. Campos), jailson_alfa@hotmail.com (J.J. da Silva), celmy@ufpe.br (C.M.B.M. Barbosa), marta.duarte@ufpe.br (M.M.M.B. Duarte)

Received 10 March 2015; Accepted 10 June 2015

ABSTRACT

Banana peel (BP) and green coconut mesocarp (GCM) were evaluated as adsorbents for the removal of the dyes reactive gray BF-2R (RG), reactive turquoise Q-G125 and remazol golden yellow RNL-150% (RGY). Adsorbents were classified as mesoporous materials, with the pHzpc of 5 for BP and 7 for GCM. The initial pH of the best-adsorbing solution of the dyes was 2.0. There was no significant difference between the kinetic models evaluated by the *F* test at a 95% level of confidence, except for the RGY/GCM system. The adsorption process is not merely a function of an intraparticle diffusion step. The Freundlich model was the best fit for RGY/GCM, and no significant difference was evident between the two models evaluated for the other systems by the *F* test. For RG/BP, the models did not fit the experimental data. The adsorbents evaluated may be useful for the treatment of effluents that contain dyes.

Keywords: Adsorption process; Kinetic study; Equilibrium study; Agro-industrial residue; Anionic dyes

1. Introduction

Textile and clothing production are the fourth largest economic activity in the world and are among the industries that consume the highest quantity of water. During the dyeing process, most of the dye is taken up by the fibre, but the fraction that is not absorbed is released with water disposal. It is estimated that 1–15% of the effluent dye is lost during the dyeing process [1].

The disposal of wastewater containing industrial dyes to rivers and lakes without proper treatment has caused many problems. Some dyes have mutagenic, carcinogenic or teratogenic properties, in addition to colouring the body of water, causing changes in appearance. Photosynthetic activities of algae and phytoplankton in lakes and rivers are also adversely affected. Furthermore, the improper wastewater disposal leads to promotion of disturbances in gas solubility, causing damage to the gills of aquatic organisms and disrupting their spawning sites and refuges [2–8].

The main processes used in the removal of dyes from wastewater from the textile industry are as follows: conventional biological treatments (activated sludge), physicochemical processes (coagulation/

*Corresponding author.

flocculation), advanced oxidation processes and membrane filtration processes. However, these technologies are not completely effective and may not have economic advantages in the treatment of target compounds because many require large areas or are limited due to the associated costs [2,9–13].

Of these treatment processes, adsorption is reported to be an effective method for removing contaminants from wastewater; it also offers the possibility of regeneration, recovery and recycling of adsorbent material; a relatively moderate cost compared to other methods of treatment; and a lower processing time with few variables that need to be controlled [3,14,15].

With the aim of reducing the environmental impacts caused by agro-industrial waste, these waste products are being employed as adsorbents in adsorption processes due to their unique chemical composition, abundance, low cost and renewable nature [11,16–23].

Bananas are one of the most consumed fruits in the world, and the peel is the main waste residue. The banana peel (BP) accounts for 30–40% of the total fruit weight and represents a major agricultural waste in banana-producing regions around the world [24–26]. Coconut shell can be readily acquired and handled, and therefore it is one of the most studied materials for reuse [16,27]. Research wastewater treatments using agro-industrial wastes as adsorbents have been adopted and encouraged [21].

Given the above conditions, the aim of this study was to evaluate adsorption processes using agro-industrial wastes as adsorbents for the removal of dyes from solutions to address environmental issues in conjunction with technological development.

2. Experimental

In this work, all reagents used for pH adjustment and for tests were of analytical grade. The dye solutions (remazol golden yellow RNL-150% (RGY), reactive gray BF-2R (RG) and reactive turquoise Q-G125 (RT)) were prepared. The colour index (CI) names, CAS Registry Number, molecular formula and molecular weight of these dyes were reported by Nascimento et al. [28].

Adsorption assays were performed in a finite bath system; at the end of each test, the samples were filtered. The concentration of the dye solution was measured before and after contact with the adsorbent using UV–vis spectrometry (Thermo Scientific, model Genesys 10S spectrometer) at a wavelength of high absorbance for each dye. Blank assays for dyes and adsorbents were also performed using the same procedure.

The amount of dye adsorbed per gram of adsorbent was calculated using Eq. (1):

$$q = \frac{(C_o - C_f)V}{M} \quad (1)$$

where q is the adsorption capacity (mg g^{-1}); C_o and C_f are the initial and final concentrations, respectively, of dye in the solution (mg L^{-1}); V is the volume of solution used (L); and M is the adsorbent mass (g).

2.1. Preparation and characterisation of the adsorbents

The BP and green coconut mesocarp (GCM) were washed with water, dried at 60°C, ground in a knife mill (Tecnal) and washed again thoroughly with distilled water, as described previously by Bhatnagar and Sillanpää [16]. After washing, samples were dried again at 60°C and classified in a series of Tyler sieves with particle sizes of <0.4 mm, 0.4–0.6 mm and 0.6–0.8 mm.

Functional groups on the surface of the adsorbent were identified with infrared spectroscopy. The absorption spectra were obtained using an infrared spectrometer (FTIR IRAffinity Shimadzu) with a diffuse reflectance accessory (Pike Technologies Inc., Model: EasiDiff TM). The spectra were recorded in the 400–4,000 cm^{-1} wavelength range.

The surface area of the material was determined by N_2 adsorption at 77 ± 5 K with a Micromeritics device (model ASAP 2420). Prior to analysis, 0.2 g of the sample was pretreated at 60°C under vacuum (DEGASS) for 3 h. This treatment was performed to remove moisture from the surface of the solid material.

The pH at the point of zero charge (pH_{zpc}) of the adsorbent was estimated by pH measurements before and after contact with the solid according to the method outlined by Regalbuto and Robles [29]. In assays, 0.25 g of the adsorbent were placed in 50 mL of H_2O, with an initial pH range of 2 to 10. The pH solution was adjusted with HCl (0.1 mol L^{-1}) or NaOH (0.1 mol L^{-1}). The solutions were agitated for 24 h and then filtered before the pH was measured. The graph of (pH_{final}–$pH_{initial}$) vs. $pH_{initial}$ was constructed, and the pH_{zpc} value was estimated from this graph where (pH_{final}–$pH_{initial}$) is zero.

2.2. Preliminary studies

The influence of the initial pH of the dye solution was evaluated using mixtures containing 0.1 g of

adsorbent in 50 mL of 100 mg L^{-1} dye solution at pH levels of 2 to 10, adjusted with solutions of HCl (0.1 mol L^{-1}) or NaOH (0.1 mol L^{-1}) and stirred at 300 rpm for 120 min.

The effect of the adsorbents' concentration was evaluated in the range of 1–60 g L^{-1}. Dye solutions with an initial concentration of 100 mg L^{-1} and a pH value determined in the initial pH study were kept in contact with the adsorbent and stirred at 300 rpm for 120 min.

To observe the influences of multiple variables on the adsorption processes and to determine the best working conditions, a 2^3 factorial design was performed with a central point in triplicate. The variables were as follows: adsorbent mass (0.25, 0.50 and 0.75 g), adsorbent particle size (<0.4, 0.4–0.6 and 0.6–0.8 mm) and stirring speed (100, 200 and 300 rpm). The variable used to determine the efficiency of the process was the adsorptive capacity (q, mg g^{-1}).

For the tests in the finite bath system, a 125 mL Erlenmeyer flask was used. The flask contained 50 mL of the dye solution at a concentration of 100 mg L^{-1} and used HCl (0.1 mol L^{-1}) for pH adjustment purposes. Assays were performed in a randomised order and at ambient room temperature (25 ± 2°C) with the aid of a shaker.

The calculations of the effects of each factor, the determination of interactions of each factor with their respective standard errors and the response surfaces corresponding to each factor were performed as described in the literature [30] using the program *Statistica for Windows* 6.0.

2.3. Study of adsorption process parameters

Kinetic and equilibrium studies were performed to determine both the time at which the system reached equilibrium and the maximum adsorption capacity of each adsorbent. These studies were based on the working conditions established by the factorial design.

Independent kinetic experiments were conducted with six concentrations of each dye and for each adsorbent, with measurements taken at intervals of 5 to 360 min. Pseudo-first-order (Eq. (2)), pseudo-second-order (Eq. (3)) and Weber–Morris (Eq. (4)) kinetic models were used:

$$\frac{dq_t}{dt} = k_1(q_e - q_t) \tag{2}$$

where k_1 is the adsorption constant of the pseudo-first-order equation (min^{-1}), q_e and q_t are the quantities of dye adsorbed (mg g^{-1}) at equilibrium and at time t, respectively;

$$\frac{dq_t}{dt} = k_2(q_e - q_t)^2 \tag{3}$$

where k_2 is the adsorption constant of the pseudo-second-order equation (g mg^{-1} min^{-1});

$$q_t = k_{dif}t^{1/2} + C \tag{4}$$

and where k_{dif} is the intraparticle diffusion coefficient (mg g^{-1} $min^{-1/2}$) and C is the constant related to diffusion resistance (mg g^{-1}).

The constant k_2 is used to calculate the initial adsorption rate h (mg g^{-1} min^{-1}) for $t \to 0$ in Eq. (5):

$$h = k_2 q_e^2 \tag{5}$$

Based on the results obtained in the kinetic studies, the Langmuir (Eq. (6)), Freundlich (Eq. (7)) and Fritz–Schlunder (Eq. (8)) adsorption models were used to evaluate the adsorption process:

$$q_e = \frac{q_{max}KC_e}{1 + KC_e} \tag{6}$$

where q_e is the amount of material adsorbed onto the solid phase at equilibrium (mg g^{-1}), q_{max} is the maximum amount of material adsorbed onto the solid phase (mg g^{-1}), K is the Langmuir constant (L mg^{-1}) and C_e is the equilibrium concentration of the adsorbate (mg L^{-1});

$$q_e = K_F(C_e)^{1/n} \tag{7}$$

where K_F is the adsorption capacity relative (mg g^{-1}) (mg $L^{-1})^{-1/n}$, $1/n$ is the intensity of adsorption;

$$q_e = \frac{K_{FS}C_e^{b_1}}{1 + aC_e^{b_2}} \tag{8}$$

and where K_{FS} (mg g^{-1}) (mg $dm^{-3})^{-b1}$ and a (mg $dm^{-3})^{-b2}$ are the constants from the Fritz–Schlunder isotherm; and b_1 and b_2 are heterogeneity factors.

The experimental data obtained from the equilibrium and kinetic studies were adjusted by mathematical models using a non-linear regression method (Origin 8.0). The model parameters were obtained by minimising the sum of the squared deviations between the experimental and predicted values. The model fit was assessed by the relative standard deviations and the regression coefficients (R^2). The

performances of the better fitting models were compared using an F test as described in the literature [31]. The critical value calculated (F_{cal}) is defined in Eq. (9):

$$F_{cal} = \frac{S_R^2(A)}{S_R^2(B)} \quad (9)$$

Here, $S_R^2(A)$ and $S_R^2(B)$ represent the variances of models A and B, respectively, with $S_R(A) > S_R(B)$. If $F_{cal} > F_{tab}$, then model B provides a better fit than model A at a 95% confidence level. F_{tab} is the critical value tabulated.

3. Results and discussion

3.1. Characterisation of the adsorbents

The origin and nature of the biosorbents, such as their physical structure, chemical nature and functional groups, may control their biosorption performance [32]. FTIR spectra of BP and GCM were obtained to understand the nature of the functional groups present in the materials.

The infrared spectra of BP and GCM are shown in (Fig. 1), and the bands found in these spectra are shown in Table 1.

The compounds found in these biomass sources are mainly cellulose, hemicellulose, pectin substances, chlorophyll pigments, and other low-molecular-weight compounds. It is believed that the adsorption characteristics of these materials are mainly due to the presence of hydroxyl and carboxyl functional groups present in pectin substances [33].

Similar results were also obtained in the literature of Albarelli et al. [24], Hameed et al. [34,35], Vieira et al. [36,37], and Amel et al. [38].

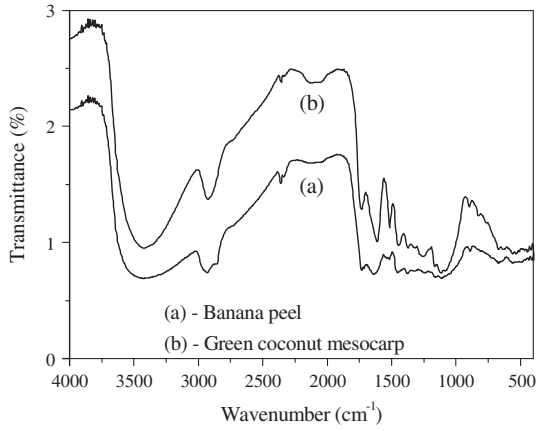

Fig. 1. Infrared spectra of BP (a) and GCM (b).

The results of textural characterisation of the adsorbents for adsorption/desorption of N_2 are shown in Table 2.

As shown in Table 2, GCM had a larger surface area and pore volume than BP; nevertheless, both had pore sizes in the range of 20–500 Å. According to the International Union of Pure and Applied Chemistry (IUPAC), these are mesoporous materials.

(Fig. 2) shows the test results carried out with the BP and GCM adsorbents in 50 mL of solution with a pH ranging from 2 to 10.

According to (Fig. 2), the pH_{zpc} of the BP was 5.0 and that of the GCM was 7.0. Below the pH_{zpc} value, a solid material has a positive surface charge, thereby promoting the adsorption of anions. Above the pH_{zpc} value, the surface is negatively charged, thereby favouring the adsorption of cations.

Similar results were obtained by Vieira et al. [36], who studied the adsorption of blue remazol (R160) into babassu coconut mesocarp and determined the

Table 1
Bands found in the infrared spectra of BP and GCM

Wavenumber (cm^{-1})		
BP	GCM	Groups/Functions
3,417.9	3,417.9	Presence of O–H groups. This band is associated with axial stretching of OH groups of cellulose, lignin and polyphenols.
2,927.9	2,925.1	C–H from methyl and methylene groups. These groups are common in the structure of lignin, cellulose and hemicellulose.
1,732.1	1,732.1	C–O stretching of carboxylic acid or ester.
1,631.8	1,612.5	Presence of conjugate C–C bond of diene.
1,111.0	1,118.7	Aromatic C–O stretching vibrations of the lignin component and –C–O–C– stretching.
910.4	925.8	Ester vibrations and mono-substituted aromatic rings due to the lignin fraction in the raw material.

Table 2
Adsorbent characterisation using the BET method

Adsorbent	Surface area ($m^2\ g^{-1}$)	Pore volume ($cm^3\ g^{-1}$)	Pore size (Å)
BP	18.6	0.02	34.9
GCM	82.0	0.07	35.8

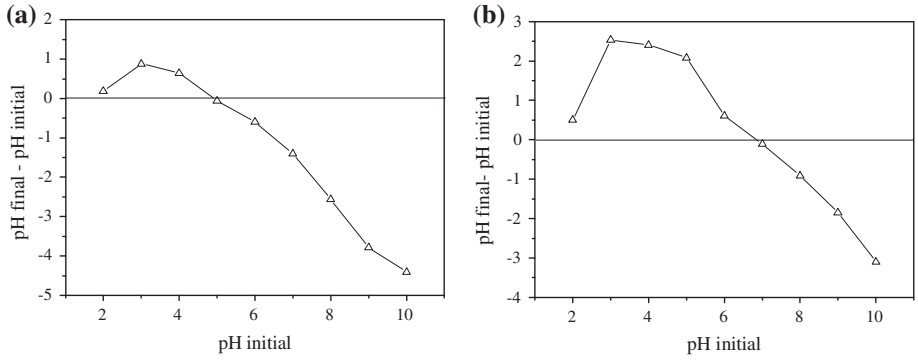

Fig. 2. pH_{zpc} of adsorbents. (a) BP and (b) GCM.

pH_{zpc} to be 6.7. Zhang et al. [39] studied the adsorption of congo red by ball-milled sugarcane bagasse and found a pH_{pzc} of 5.0.

3.2. Preliminary studies

The influence of the initial pH of the dye solution was investigated by comparing the adsorption capacity of the adsorbents at pH 2–10, as shown in (Fig. 3).

In the pH studies, it was observed that the dye adsorption performance was affected by the initial pH of the solution, with smaller values of q at more basic pH values, presumably due to electrostatic repulsion. The highest adsorption capacity for all dyes and adsorbents evaluated was observed at pH 2.

Aksu and Isoglu [40] studied the effect of pH solution on the adsorption of the reactive dye remazol turquoise blue-G using sugar beet pulp; the adsorption reached a maximum at pH 2.

According to Wang [13], adsorbents maintain a net positive charge when the pH solution is lower than pH_{pzc}. As a result, an electrostatic interaction occurs between the negatively charged dye molecules and the positively charged adsorption sites on the adsorbent. At low pH, the electrostatic attraction is significantly higher, thereby causing an increase in dye adsorption. This phenomenon at low pH is due to an increase in the number of protonated species on the surface of the adsorbent, including carboxylic, phenolic and chromenic groups.

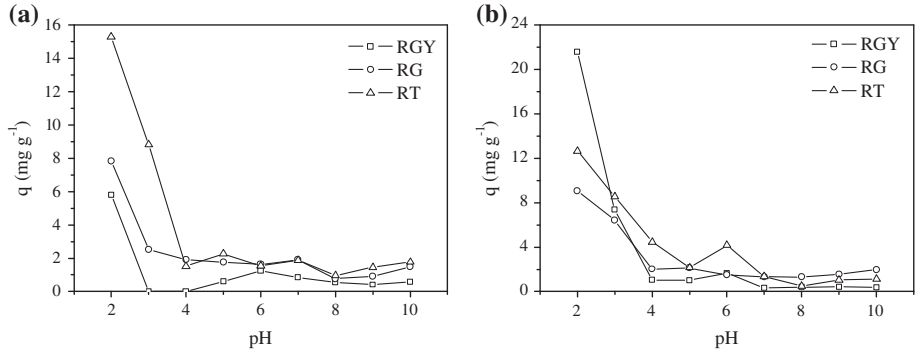

Fig. 3. Effect of pH on the adsorption capacities of adsorbents. (a) BP and (b) GCM.

Table 3
Relationship between the minimum and maximum adsorption capacities, and the minimum and maximum percentage removals obtained in the adsorbent concentration study

	RGY/BP		RGY/GCM		RG/BP		RG/GCM		RT/BP		RT/GCM	
Adsorbent concentration (g L^{-1})	4	40	4	40	4	40	4	40	4	40	4	40
q (mg g^{-1})	7.8	2.5	6.8	1.1	1.8	1.2	4.8	1.6	5.6	0.9	4.1	1.0
% removal	11.1	70.2	9.6	94.9	14.0	75.4	38.0	100	54.7	100	34.2	96.6

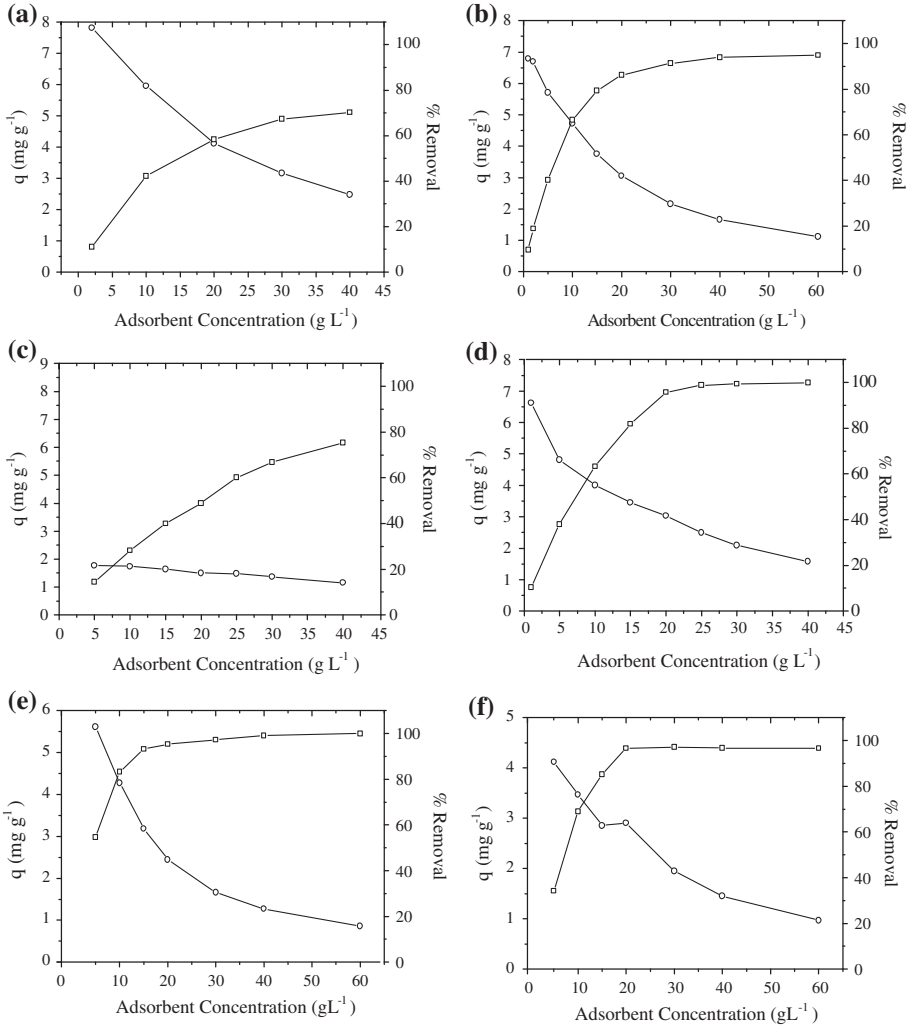

Fig. 4. The effect of varying the concentration of adsorbents used for dye adsorption. (a) RGY/BP; (b) RGY/GCM; (c) RG/BP; (d) RG/GCM; (e) RT/BP and (f) RT/GCM. ▫: % dye removal and ○: q (mg g^{-1}).

Table 3 shows the minimum and maximum of both adsorption capacity and percentage removal obtained in the adsorbent concentration study.

Similar behaviour was observed by Ertaş et al. [41] in a study of the biosorbents cotton stalk, cotton waste and cotton dust for the removal of methylene blue. It was shown that when the adsorbent dose increased from 0.25 to 1.50 g, the percentage of dye removal by cotton stalk, cotton waste and cotton dust increased from 35.08 to 48.36%, from 68.03 to 85.41% and from

Table 4
Main and interaction effects and their standard errors. Statistically significant effects, at the 95% confidence level, are shown in boldface

Effect	Estimates					
	RGY/BP	RGY/GCM	RG/BP	RG/GCM	RT/BP	RT/GCM
Mean	3.86 ± 0.04	4.612 ± 0.005	4.01 ± 0.05	3.39 ± 0.01	3.807 ± 0.007	4.15 ± 0.02
Principal effects						
Mass (M)	**−2.43 ± 0.08**	**−2.24 ± 0.01**	**−2.2 ± 0.1**	**−1.15 ± 0.02**	**−2.72 ± 0.02**	**−2.34 ± 0.03**
Particle Size (PS)	**−0.76 ± 0.08**	**−0.46 ± 0.01**	−0.2 ± 0.1	**−0.81 ± 0.02**	**−0.29 ± 0.02**	**−2.61 ± 0.03**
Stirring Speed (SS)	**1.87 ± 0.08**	**0.77 ± 0.01**	**2.0 ± 0.1**	**1.21 ± 0.02**	**1.79 ± 0.02**	**2.04 ± 0.03**
Effects of interaction						
M vs. PS	**0.41 ± 0.08**	**0.08 ± 0.01**	0.4 ± 0.1	**0.46 ± 0.02**	**0.34 ± 0.02**	**1.42 ± 0.03**
M vs. SS	**−0.79 ± 0.08**	**−0.30 ± 0.01**	**−1.2 ± 0.1**	**−0.30 ± 0.02**	**−0.56 ± 0.02**	**−0.99 ± 0.03**
PS vs. SS	−0.12 ± 0.08	**−0.60 ± 0.01**	**0.9 ± 0.1**	**0.16 ± 0.02**	**−0.13 ± 0.02**	**−0.90 ± 0.03**
M vs. PS vs. SS	0.02 ± 0.08	**0.52 ± 0.01**	**−1.1 ± 0.1**	**−0.17 ± 0.02**	0.07 ± 0.02	**0.98 ± 0.03**
t_s vs. s	0.34	0.04	0.4	0.09	0.09	0.13

83.93 to 91.47%, respectively, at an equilibrium time of 90 min. However, unit adsorption, indicating the amount of solute adsorbed per unit adsorbent, decreased with an increase in adsorbent dose. For example, when the adsorbent dosage increased from 0.25 to 1.50 g, the values of unit adsorption for cotton stalk, cotton waste and cotton dust decreased from 3.51 to 0.81 mg g^{-1}, from 6.80 to 1.42 mg g^{-1} and from 8.39 to 1.52 mg g^{-1}, respectively.

The effect of varying the concentration of adsorbents used for dye adsorption is shown in (Fig. 4).

A previous investigation of the effect of mass on the removal of indigo carmine by rice husk ash showed that the indigo carmine removal increased up to a certain limit and then remained almost constant. An increase in adsorption with increasing adsorbent dose can be attributed to greater surface area and the availability of more adsorption sites. Furthermore, in

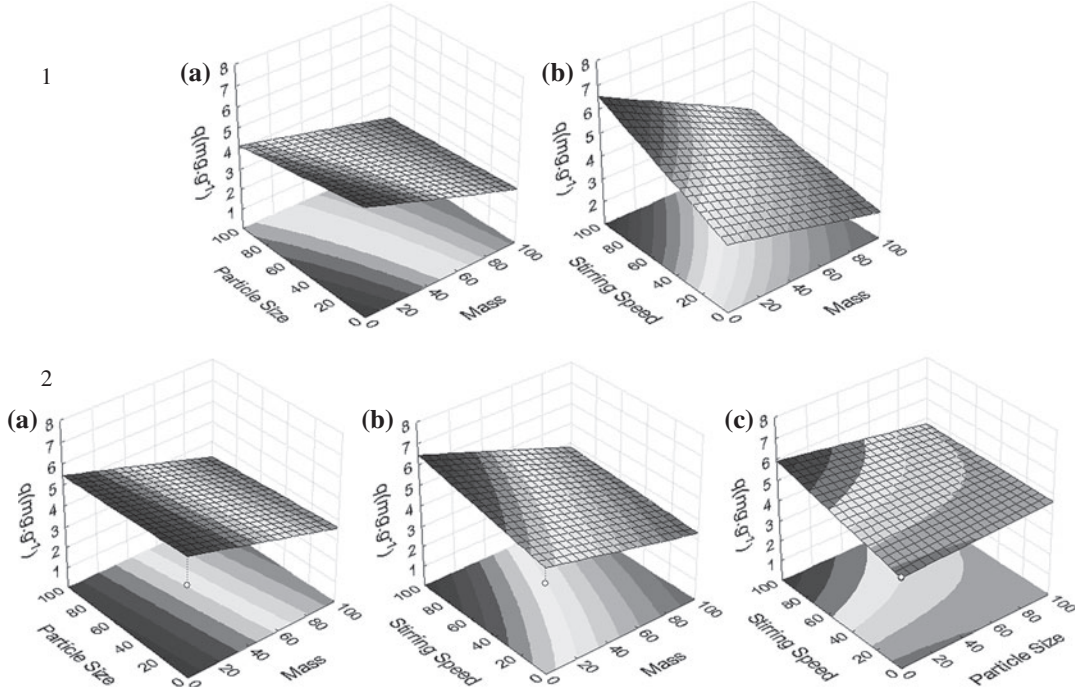

Fig. 5. Response surfaces for adsorption capacity. (1) RGY/BP and (2) RGY/GCM. (a) Mass vs. Particle Size; (b) Mass vs. Stirring Speed and (c) Particle Size vs. Stirring Speed.

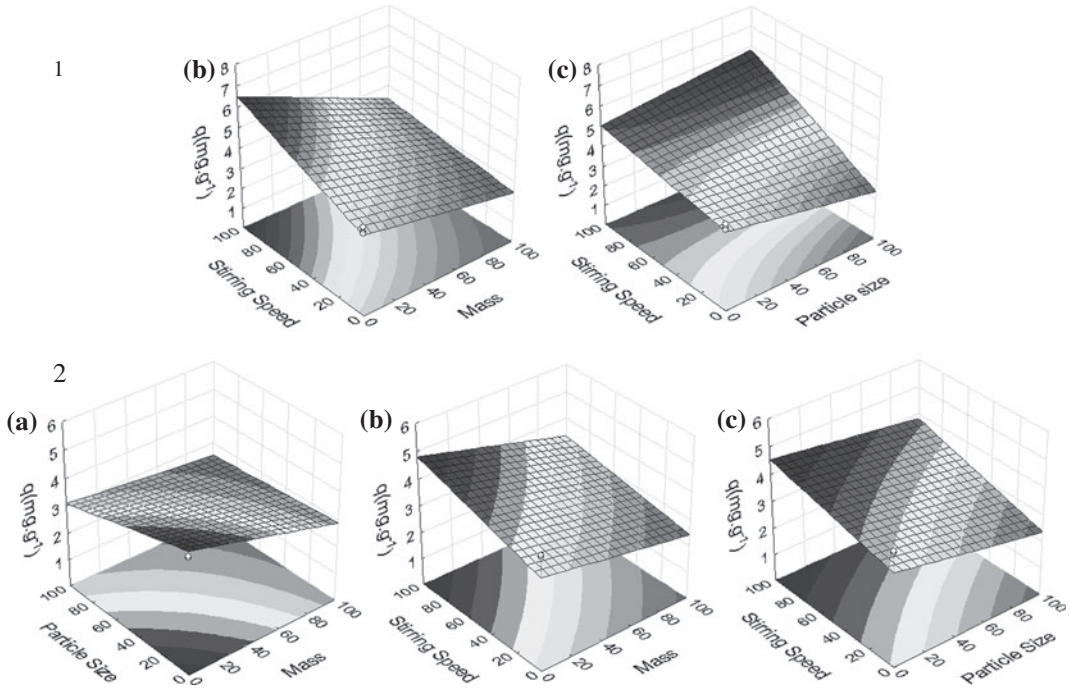

Fig. 6. Response surfaces for adsorption capacity. (1) RG/BP and (2) RG/GCM. (a) Mass vs. Particle Size; (b) Mass vs. Stirring Speed; (c) Particle Size vs. Stirring Speed.

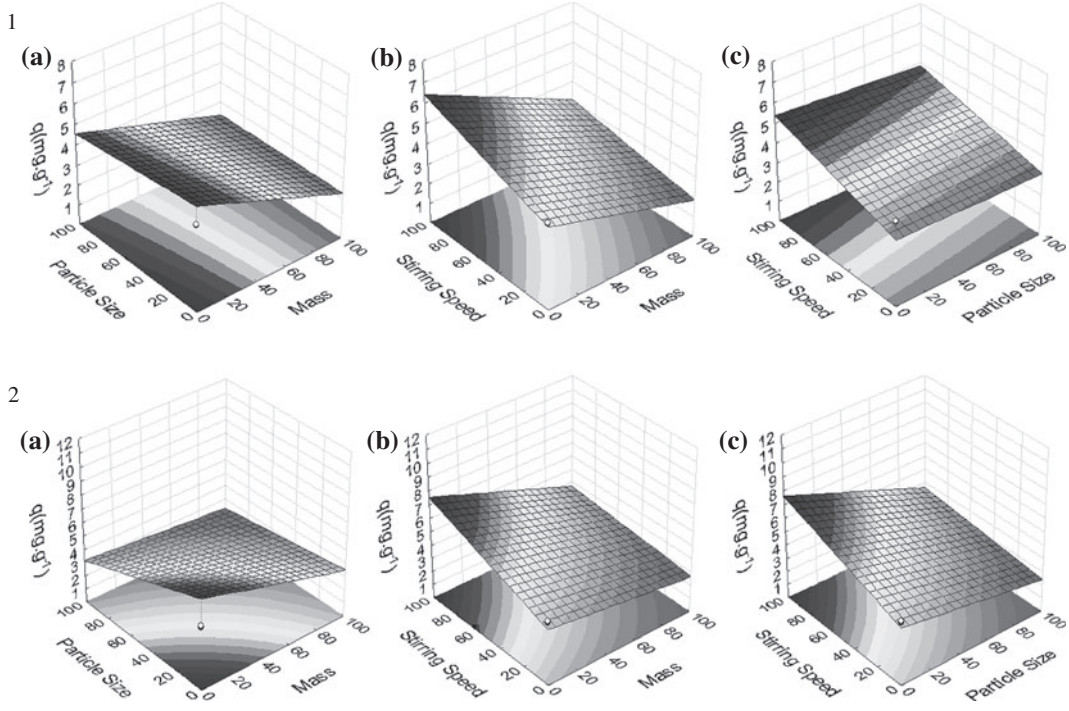

Fig. 7. Response surfaces for adsorption capacity. (1) RT/BP and (2) RT/GCM. (a) Mass vs. Particle Size; (b) Mass vs. Stirring Speed; (c) Particle Size vs. Stirring Speed.

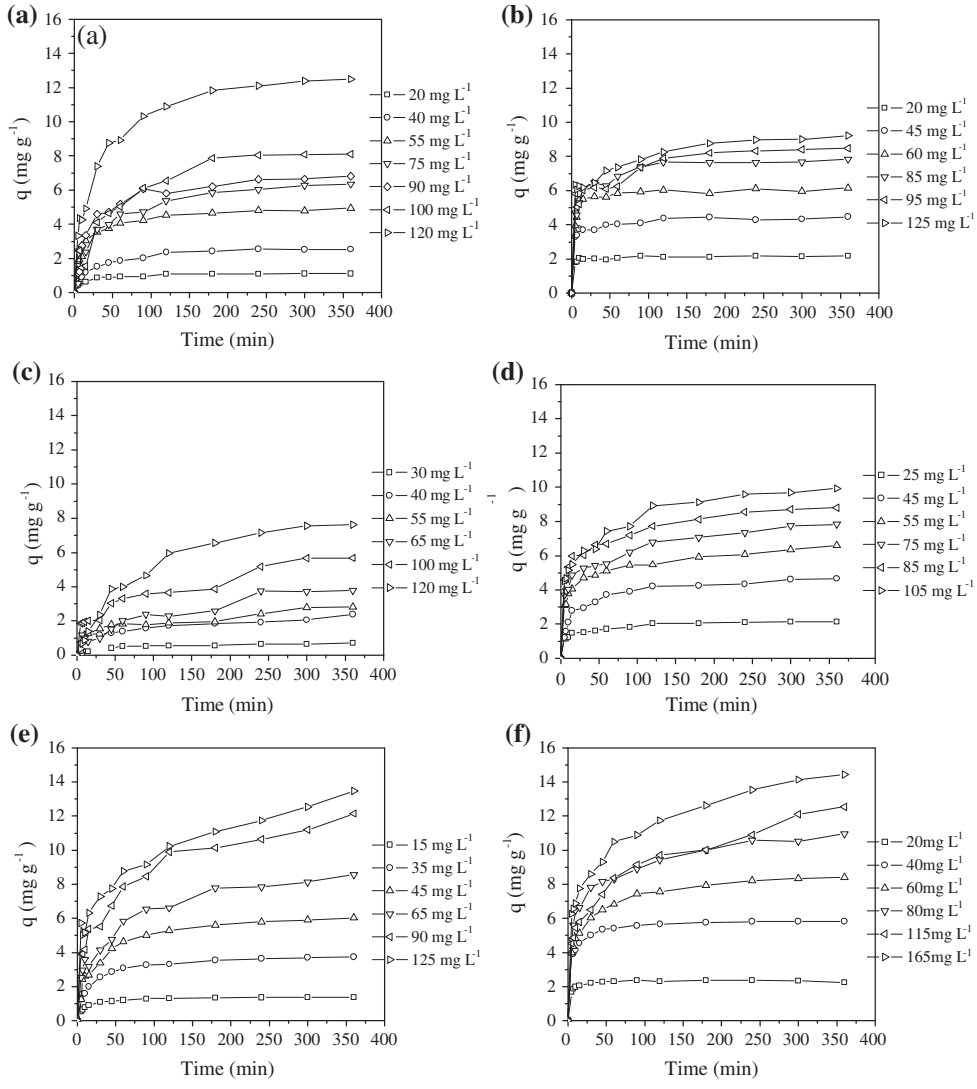

Fig. 8. Adsorption kinetics in finite bath system: (a) RGY/BP; (b) RGY/GCM; (c) RG/BP; (d) RG/GCM; (e) RT/BP and (f) RT/GCM. Tests carried out at pH 2.0, SS = 300 rpm, PS = < 0.4 mm and M = 0.25 g for 100 mL of solution.

all cases, sorption was attained more rapidly at a lower adsorbent dosage [17], as shown in (Fig. 4).

The mass corresponding to the intersection of the curves in (Fig. 4) was used as a central point for the factorial design to find the best value of percentage removal vs. adsorptive capacity.

Using the data obtained with the completion of the 2^3 factorial design and the software *Statistica for Windows* version 6.0, main and interaction effects were calculated and are presented in Table 4. The effects considered statistically significant at a 95% level of confidence were those that extend student t vs. standard errors (t_s vs. s).

As shown in Table 4, all of the effects were statistically significant at a 95% confidence level, except for the interaction effects of particle size vs. stirring speed for RGY/BP, the interaction of all three factors for RGY/BP and the effects of particle size and mass vs. particle size for RG/BP.

The mass effect was the most important for BP and RGY/GCM. The principal effects, which were stirring speed and particle size, were the most important for RG/GCM and RT/GCM, respectively.

Significant interaction effects were observed at a 95% confidence level, which means that the adsorbent mass, particle size and stirring speed variables cannot be independently evaluated.

The response surfaces for the interactions of different pairs of statistically significant factors are presented in Figs. 5, 6 and 7.

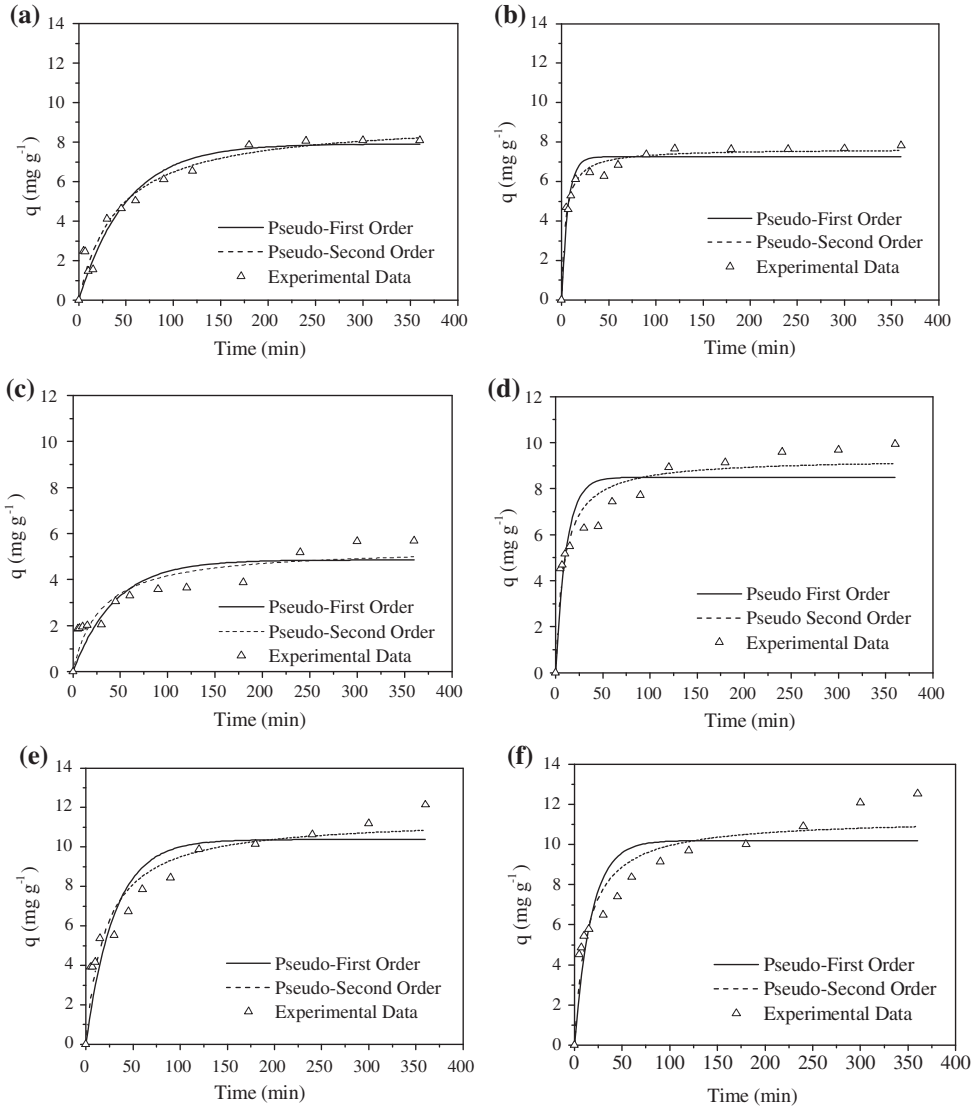

Fig. 9. Nonlinear fittings of kinetic models. (a) RGY/BP; (b) RGY/GCM; (c) RG/BP; (d) RG/GCM; (e) RT/BP and (f) RT/GCM.

It can be observed in Figs. 5, 6 and 7 that the highest adsorption capacity q (mg g^{-1}) was obtained for a lower adsorbent mass (0.25 g), for a small particle size (<0.4 mm) and for the highest stirring speed (300 rpm).

Based on these results, another factorial design experiment was conducted with a mass of 0.25 g and a lower stirring speed of 300 rpm; however, the reproducibility of the results was compromised due to the small mass of adsorbent material available in solution. At higher stirring speeds, the adsorbent was pushed to the walls of the flask, reducing the contact of the liquid–solid system and, consequently, the adsorption capacity.

3.3. Study of adsorption process parameters

Fig. 8 shows a plot of the kinetic adsorption data for the RGY, RG and RT dyes in the solid phase using the BP and GCM adsorbents.

It was found that the kinetics evolved rapidly during the first few minutes, removing most of the dye in approximately 30 min, as expected from a good adsorbent. This was followed by a slow phase equilibrium which was reached after a maximum of 180 min for the adsorbents studied.

The nonlinear fittings of pseudo-first-order and pseudo-second-order kinetic models for the experimental data are shown in (Fig. 9).

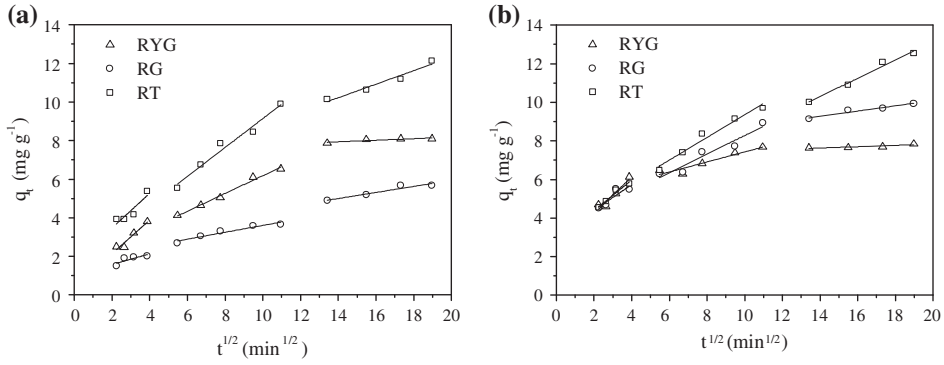

Fig. 10. Intraparticle diffusion Weber–Morris model. (a) BP e (b) GCM.

As shown in (Fig. 9), using the models given in Table 5 and the results obtained from the F test (F_{cal} (Table 5) > F_{tab} (2.69)), assuming a confidence level of 95%, the pseudo-second-order model showed a better fit to the experimental data for only the RGY/GCM system. For the RGY/BP, RG/GCM, RT/BP and RT/GCM systems, no significant difference was observed between the two models. Fig. 9(c) shows that neither model fit the experimental data for the RG/BP system.

The kinetics results obtained here are corroborated by Saeed et al. [42], who studied the removal of crystal violet dye using grape skin as an adsorbent. The adsorption kinetics showed that the system reached equilibrium at 100 min and that the pseudo-second-order model was best suited to the data obtained.

The kinetics data were also analysed to determine whether the intraparticle diffusion rate is the limiting step of adsorption. In this study, the linear regression by parts method was used for data adjustment, as shown in (Fig. 10).

The Weber–Morris equation did not satisfy a linear relationship with the experimental data, which was multilinear. This result, as Lakshmi et al. [17] demonstrated, indicates that the adsorption process is not merely controlled by an intraparticle diffusion step. This implies that two or more steps control the process.

The intraparticle diffusion parameters for the regions, k_{dif1}, k_{dif2} and k_{dif3}, were determined from the slope of the plotted graph (Fig. 10). The differences in the diffusion rate parameter between the three regions is attributed to macropore diffusion, transitional pore diffusion and micropore diffusion ($k_{dif1} > k_{dif2} > k_{dif3}$, Table 6) [43].

The values of C give an indication of the boundary layer thickness. For instance, at a higher value of C,

Table 5
Parameters for the kinetic models of dye adsorption obtained for concentration of 100 mg L^{-1}

	RGY/BP	RGY/GCM	RG/BP	RG/GCM	RT/BP	RT/GCM
Pseudo-first-order						
R^2	0.929	0.930	0.746	0.814	0.852	0.802
k_1 (min^{-1})	0.019 ± 0.003	0.15 ± 0.02	0.023 ± 0.06	0.09 ± 0.02	0.033 ± 0.007	0.06 ± 0.01
$q_{e,calc}$ (mg g^{-1})	7.9 ± 0.4	7.2 ± 0.2	4.8 ± 0.4	8.5 ± 0.4	10.4 ± 0.6	10.2 ± 0.6
S_R^2 (mg^2 g^{-2})	6.69	3.69	8.18	16.76	21.71	27.86
Pseudo-second-order						
R^2	0.929	0.976	0.761	0.919	0.929	0.907
k_2 (g(mgmin)$^{-1}$)	0.0265 ± 0.0007	0.031 ± 0.004	0.006 ± 0.003	0.012 ± 0.003	0.004 ± 0.001	0.006 ± 0.002
$q_{e,calc}$ (mg g^{-1})	9.1 ± 0.5	7.7 ± 0.1	5.4 ± 0.5	9.3 ± 0.4	11.5 ± 0.5	11.3 ± 0.5
h (mgg^{-1} min^{-1})	0.25	1.76	0.17	1.04	0.53	0.77
S_R^2 (mg^2 g^{-2})	5.02	1.27	5.35	7.33	10.36	13.00
$q_{e,exp}$.(mg g^{-1})	8.1	7.7	5.7	9.7	11.2	12.1
F_{cal}	1.33	2.91	1.53	2.29	2.09	2.14

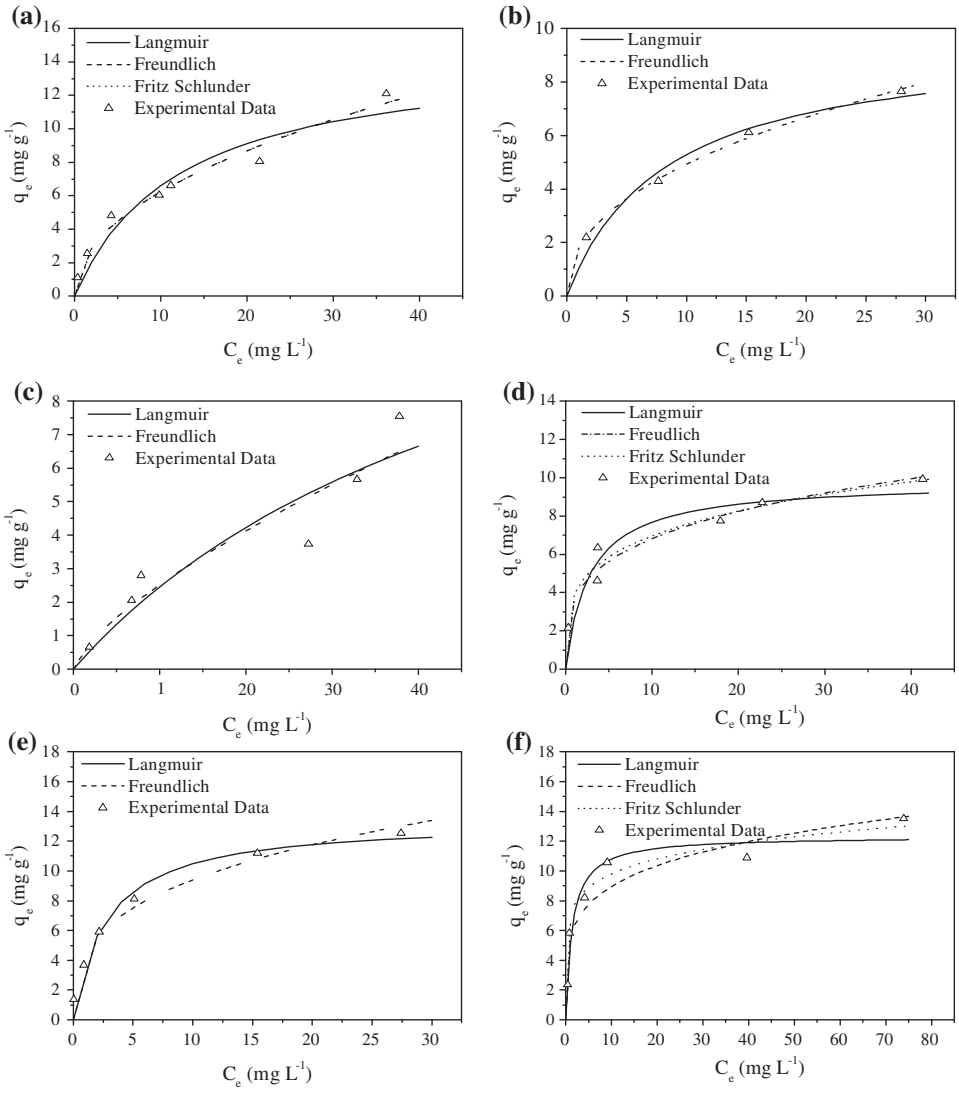

Fig. 11. Dye adsorption isotherms. (a) RGY/BP; (b) RGY/GCM; (c) RG/BP; (d) RG/GCM; (e) RT/BP and (f) RT/GCM.

Table 6
Intraparticle diffusion Weber–Morris model constants

Parameters	RGY/BP	RGY/GCM	RG/BP	RG/GCM	RT/BP	RT/GCM
$k_{dif,1}$ mg(g min$^{1/2}$)$^{-1}$	0.874 ± 0.165	0.952 ± 0.214	0.277 ± 0.129	0.663 ± 0.231	0.902 ± 0.283	0.788 ± 0.096
C_1 (mg g^{-1})	0.384 ± 0.051	2.329 ± 0.651	1.018 ± 0.394	3.077 ± 0.702	1.661 ± 0.859	2.812 ± 0.292
R_1^2	0.900	0.862	0.543	0.707	0.754	0.957
$k_{dif,2}$ mg(g min$^{1/2}$)$^{-1}$	0.461 ± 0.029	0.259 ± 0.049	0.179 ± 0.028	0.481 ± 0.076	0.751 ± 0.074	0.585 ± 0.062
C_2 (mg g^{-1})	1.565 ± 0.241	4.830 ± 0.414	1.812 ± 0.231	3.461 ± 0.630	1.632 ± 0.616	3.495 ± 0.512
R_2^2	0.984	0.866	0.910	0.907	0.962	0.957
$k_{dif,3}$ mg(g min$^{1/2}$)$^{-1}$	0.041 ± 0.013	0.034 ± 0.014	0.157 ± 0.032	0.136 ± 0.024	0.351 ± 0.054	0.473 ± 0.046
C_3 (mg g^{-1})	7.359 ± 0.223	7.155 ± 0.227	2.798 ± 0.532	7.374 ± 0.394	5.309 ± 0.896	3.667 ± 0.757
R_3^2	0.729	0.624	0.882	0.912	0.931	0.972

Table 7
Isotherm parameters of the Langmuir, Freundlich and Fritz–Schlunder models calculated for the adsorbents used

Models	RGY/BP	RGY/GCM	RG/BP	RG/GCM	RT/BP	RT/GCM
Langmuir						
R^2	0.912	0.951	0.826	0.879	0.972	0.904
q_{max} (mg g^{-1})	14.7 ± 2.5	9.6 ± 1.2	15.5 ± 1.6	9.8 ± 0.9	13.4 ± 0.8	12.3 ± 0.9
K (L mg^{-1})	0.08 ± 0.03	0.12 ± 0.04	0.02 ± 0.02	0.4 ± 0.1	0.36 ± 0.08	0.7 ± 0.2
S_R^2 (mg^2 g^{-2})	5.78	0.54	4.4	3.9	2.1	6.2
Freundlich						
R^2	0.974	0.995	0.855	0.939	0.985	0.835
K_F (mg g^{-1})(mg $L^{-1})^{-1/n}$	2.1 ± 0.3	1.8 ± 0.1	0.5 ± 0.3	3.6 ± 0.4	4.5 ± 0.3	5.5 ± 0.9
N	2.1 ± 0.2	2.3 ± 0.1	1.4 ± 0.4	3.7 ± 0.5	3.1 ± 0.2	4.8 ± 1.1
S_R^2 (mg^2 g^{-2})	1.69	0.05	3.6	2.0	1.2	10.6
Fritz–Schlunder						
R^2	0.957	–	–	0.903	–	0.928
K_{FS} (mg g^{-1})(mg $dm^{-3})^{-b}{}_1$	2.2 ± 0.9	–	–	409 ± 164	–	86.4 ± 7.7
a (mg $dm^{-3})^{-b}{}_2$	0.08	–	–	103.9	–	12.3
b_1	0.5	–	–	3.4	–	3.9
b_2	0.001	–	–	3.1	–	3.8
S_R^2 (mg^2 g^{-2})	1.69	–	–	1.6	–	2.3
F_{cal}	3.4	10.8	1.2	2.4	1.7	4.6

Table 8
Previous studies for anionic dye adsorption by banana and coconut wastes

Adsorbent	Dye name	q_{max} (mg g^{-1})	Reference
Babassu coconut mesocarp	Rubi S2G	1.7	Vieira et al. [36]
Green coconut mesocarp	Remazol Black B	2.9	Leal et al. [46]
Banana peel	Methyl orange	21.0	Annadurai et al. [47]
Banana peel	Congo red	18.2	Annadurai et al. [47]
Banana pith	Acid brilliant blue	4.42	Namasivayam et al. [48]
Green coconut mesocarp	Remazol golden yellow RNL-150%	9.6	This work
Green coconut mesocarp	Reactive gray BF-2R	9.8	This work
Green coconut mesocarp	RT	12.3	This work
Banana peel	Remazol golden yellow RNL-150%	14.7	This work
Banana peel	Reactive gray BF-2R	15.5	This work
Banana peel	RT	13.4	This work

the effect of the boundary layer is more significant. When the values of C are nonzero, this indicates that the line as plotted on the graph q_t vs. $t^{1/2}$ (Fig. 10) does not pass through the origin. Therefore, the mechanism of intraparticle diffusion is not the determining step in the process of mass transfer; rather, other mechanisms must operate simultaneously to control the adsorption process [44].

The adsorption models were applied to the experimental data over the time range of 0–240 min to ensure that equilibrium had been reached in the system.

The nonlinear fit of the Langmuir, Freundlich and Fritz–Schlunder models to dye removal is shown in Fig. 11.

The experimental results indicated a favourable adsorption of the dyes for the adsorbents studied.

The results of the F test (F_{cal} (Table 7) < F_{tab} (5.05)), assuming a confidence level of 95%, showed no significant difference for the models as evaluated for each system, with the exception of the RGY/GCM system. The best fit was the Freundlich model. For the RG/BP system, none of the three models fit the experimental data.

Although GCM had a greater surface area and pore volume, it can be observed in Table 7 that BP showed a higher adsorptive capacity for the dyes evaluated under the conditions studied. The smaller adsorptive capacity could be due to the structure of GCM, which has a greater number of phenolic and carboxylate functional groups than BP according to FTIR analysis.

The carboxyl group is one of the functional groups available in many agricultural waste products, affecting the adsorption capacity for some classes of dyes. The carboxyl group has a negative charge and is therefore an important functional group in the adsorption of cationic dyes. Moreover, the carboxyl groups inhibit the adsorption of anionic dyes.

The interaction between the dye molecules and these functional groups can follow an extremely complex pattern. Zhang et al. [45] related the differences in adsorption performances among dyes to the molecular structure of the dyes and the surface chemistry of the adsorbent, as is also observed in this work.

Table 8 shows the results obtained in previous studies for anionic dye adsorption using banana and coconut wastes.

Table 8 compares the adsorption capacity of banana and coconut wastes for different types of dye. The most important parameter to compare is the q_{max} value because it is a measure of the adsorption capacity of the adsorbent. The values of q_{max} in this study are within the range of values reported in the literature for the adsorption of anionic dyes onto banana and coconut wastes.

Importantly, these adsorbent materials were used without any physical or chemical pretreatment and are organic residues available worldwide.

4. Conclusion

The adsorbents studied in this work, which were prepared from agro-industrial wastes, may be viable alternatives for the removal of the RGY, RG and reactive turquoise Q-G 125 dyes from aqueous solutions. These materials possess several advantages, such as a low commercial value (because they are considered waste), abundant availability and good adsorption capacity.

Acknowledgements

Financial support was provided by the Conselho Nacional de Desenvolvimento Científico e Tecnológico (CNPq), Texpal provided the dyes, the scholarship programmes PIBIC/UFPE and PIBIC/FACEPE provided funding through IC grants, and the Centro de Tecnologias Estratégicas do Nordeste (CETENE) provided help on the characterisation of adsorbents.

List of symbols

$1/n$	—	intensity of adsorption
a	—	constant of Fritz–Schlunder $[mg\ dm^{-3}]^{-b2}$
b_1	—	factor of heterogeneity
b_2	—	factor of heterogeneity
C	—	constant related to diffusion resistance $[mg\ g^{-1}]$
C_e	—	equilibrium concentration
C_f	—	final concentration $[mg\ L^{-1}]$
C_o	—	initial concentration $[mg\ L^{-1}]$
F_{cal}	—	F calculated for the test F
F_{tab}	—	F tabulated for the test F
h	—	initial adsorption rate $(mg\ g^{-1}\ min^{-1})$
K	—	Langmuir constant $[L\ mg^{-1}]$
k_1	—	adsorption constant of the pseudo-first-order equation $[min^{-1}]$
k_2	—	adsorption constant of the pseudo-second-order equation $[g\ mg^{-1}\ min^{-1}]$
k_{dif}	—	intraparticle diffusion coefficient $[mg\ g^{-1}\ min^{-1/2}]$
K_F	—	adsorption capacity related to the Freundlich isotherm $[mg\ g^{-1}]$ $[mg\ L^{-1}]^{-1/n}$
K_{FS}	—	constant of Fritz–Schlunder $[mg\ g^{-1}]$ $[mg\ dm^{-3}]^{-b1}$
M	—	adsorbent mass [g]
q	—	adsorption capacity $[mg\ g^{-1}]$
q_e	—	adsorption capacity at equilibrium $[mg\ g^{-1}]$
$q_{e,cal}$	—	calculated adsorption capacity at equilibrium $[mg\ g^{-1}]$
$q_{e,exp}$	—	experimental adsorption capacity at equilibrium $[mg\ g^{-1}]$
q_{max}	—	maximum adsorption capacity $[mg\ g^{-1}]$
q_t	—	adsorption capacity at time t $[mg\ g^{-1}]$
R^2	—	regression coefficient
s	—	standard errors
$S_R^2(A)$	—	deviation of model A $[mg^2\ g^{-2}]$
$S_R^2(B)$	—	deviation of model B $[mg^2\ g^{-2}]$
t	—	time [min]
t_s	—	student t
V	—	volume of solution [L]
σ_i	—	relative standard deviation

References

[1] N. Barka, M. Abdennouri, M.E.L. Makhfouk, Removal of Methylene Blue and Eriochrome Black T from aqueous solutions by biosorption on *Scolymus hispanicus* L.: Kinetics, equilibrium and thermodynamics, J. Taiwan Inst. Chem. Eng. 42 (2011) 320–326.

[2] R. Ahmad, Studies on adsorption of crystal violet dye from aqueous solution onto coniferous pinus bark powder (CPBP), J. Hazard. Mater. 171 (2009) 767–773.

[3] V.K. Gupta, Suhas, Application of low-cost adsorbents for dye removal—A review, J. Environ. Manage. 90 (2009) 2313–2342.

[4] B.H. Hameed, A.A. Ahmad, Batch adsorption of methylene blue from aqueous solution by garlic peel, an agricultural waste biomass, J. Hazard. Mater. 164 (2009) 870–875.

[5] K. Kadirvelu, M. Kavipriya, C. Karthika, M. Radhika, N. Vennilamani, S. Pattabhi, Utilization of various agricultural wastes for activated carbon preparation and application for the removal of dyes and metal ions from aqueous solutions, Bioresour. Technol. 87 (2003) 129–132.

[6] D.K. Mahmoud, M.A.M. Salleh, W.A.W.A. Karim, A. Idris, Z.Z. Abidin, Batch adsorption of basic dye using acid treated kenaf fibre char: Equilibrium, kinetic and thermodynamic studies, Chem. Eng. J. 181–182 (2012) 449–457.

[7] C.-Y. Tan, M. Li, Y.-M. Lin, X.-Q. Lu, Z.-L. Chen, Biosorption of Basic Orange from aqueous solution onto dried *A. filiculoides* biomass: Equilibrium, kinetic and FTIR studies, Desalination 266 (2011) 56–62.

[8] T. Wang, K. Kailasam, P. Xiao, G. Chen, L. Chen, L. Wang, J. Li, J. Zhu, Adsorption removal of organic dyes on covalent triazine framework (CTF), Microporous Mesoporous Mater. 187 (2014) 63–70.

[9] S. Jain, R.V. Jayaram, Removal of basic dyes from aqueous solution by low-cost adsorbent: Wood apple shell (*Feronia acidissima*), Desalination 250 (2010) 921–927.

[10] R. Kumar, R. Ahmad, Biosorption of hazardous crystal violet dye from aqueous solution onto treated ginger waste (TGW), Desalination 265 (2011) 112–118.

[11] M.S. Sajab, C.H. Chia, S. Zakaria, P.S. Khiew, Cationic and anionic modifications of oil palm empty fruit bunch fibers for the removal of dyes from aqueous solutions, Bioresour. Technol. 128 (2013) 571–577.

[12] M.T. Sulak, E. Demirbas, M. Kobya, Removal of Astrazon Yellow 7GL from aqueous solutions by adsorption onto wheat bran, Bioresour. Technol. 98 (2007) 2590–2598.

[13] L. Wang, Application of activated carbon derived from 'waste' bamboo culms for the adsorption of azo disperse dye: Kinetic, equilibrium and thermodynamic studies, J. Environ. Manage. 102 (2012) 79–87.

[14] E. Eren, O. Cubuk, H. Ciftci, B. Eren, B. Caglar, Adsorption of basic dye from aqueous solutions by modified sepiolite: Equilibrium, kinetics and thermodynamics study, Desalination 252 (2010) 88–96.

[15] M.L. Soto, A. Moure, H. Domínguez, J.C. Parajó, Recovery, concentration and purification of phenolic compounds by adsorption: A review, J. Food Eng. 105 (2011) 1–27.

[16] A. Bhatnagar, M. Sillanpää, Utilization of agro-industrial and municipal waste materials as potential adsorbents for water treatment—A review, Chem. Eng. J. 157 (2010) 277–296.

[17] U.R. Lakshmi, V.C. Srivastava, I.D. Mall, D.H. Lataye, Rice husk ash as an effective adsorbent: Evaluation of adsorptive characteristics for Indigo Carmine dye, J. Environ. Manage. 90 (2009) 710–720.

[18] G.E. Nascimento, M.M.M.B. Duarte, N.F. Campos, C.M.B.M. Barbosa, V.L. Silva, Adsorption of the reactive gray BF-2R dye on orange peel: kinetics and equilibrium studies, Desalin. Water Treat. 52 (2013) 1578–1588.

[19] S. Rangabhashiyam, N. Anu, N. Selvaraju, Sequestration of dye from textile industry wastewater using agricultural waste products as adsorbents, J. Environ. Chem. Eng. 1 (2013) 629–641.

[20] S. Sadaf, H.N. Bhatti, Batch and fixed bed column studies for the removal of Indosol Yellow BG dye by peanut husk, J. Taiwan Inst. Chem. Eng. 45 (2014) 541–553.

[21] M.A.M. Salleh, D.K. Mahmoud, W.A.W.A. Karim, A. Idris, Cationic and anionic dye adsorption by agricultural solid wastes: A comprehensive review, Desalination 280 (2011) 1–13.

[22] L. Zhou, J. Huang, B. He, F. Zhang, H. Li, Peach gum for efficient removal of methylene blue and methyl violet dyes from aqueous solution, Carbohydr. Polym. 101 (2014) 574–581.

[23] C.-H. Weng, Y.-T. Lin, T.-W. Tzeng, Removal of methylene blue from aqueous solution by adsorption onto pineapple leaf powder, J. Hazard. Mater. 170 (2009) 417–424.

[24] J.Q. Albarelli, R.B. Rabelo, D.T. Santos, M.M. Beppu, M.A.A. Meireles, Effects of supercritical carbon dioxide on waste banana peels for heavy metal removal, J. Supercrit. Fluids 58 (2011) 343–351.

[25] S.R.R. Comim, K. Madella, J.V. Oliveira, S.R.S. Ferreira, Supercritical fluid extraction from dried banana peel (*Musa* spp., genomic group AAB): Extraction yield, mathematical modeling, economical analysis and phase equilibria, J. Supercrit. Fluids 54 (2010) 30–37.

[26] H.S. Oberoi, P.V. Vadlani, L. Saida, S. Bansal, J.D. Hughes, Ethanol production from banana peels using statistically optimized simultaneous saccharification and fermentation process, Waste Manage. 31 (2011) 1576–1584.

[27] A. Bhatnagar, V.J.P. Vilar, C.M.S. Botelho, R.A.R. Boaventura, Coconut-based biosorbents for water treatment—A review of the recent literature, Adv. Colloid Interface Sci. 160 (2010) 1–15.

[28] G.E. Nascimento, M.M.M.B. Duarte, N.F. Campos, O.R.S. Rocha, V.L. Silva, Adsorption of azo dyes using peanut hull and orange peel: A comparative study, Environ. Technol. 35 (2014) 1436–1453.

[29] J.R. Regalbuto, J. Robles, The engineering of Pt/Carbon Catalyst Preparation, University of Illinois, Chicago, IL, 2004.

[30] B. Barros Neto, I.S. Scarminio, R.E. Bruns, Como Fazer Experimentos: Pesquisa e desenvolvimento na ciência e na indústria, third ed., Unicamp, Campinas, 2007.

[31] D.C. Montgomery, Introduction to Statistical Quality Control, fourth ed., John Wiley & Sons, New York, NY, 2001.
[32] J. Gao, Q. Zhang, K. Su, R. Chen, Y. Peng, Biosorption of Acid Yellow 17 from aqueous solution by non-living aerobic granular sludge, J. Hazard. Mater. 174 (2010) 215–225.
[33] M. Thirumavalavan, Y.-L. Lai, L.-C. Lin, J.-F. Lee, Cellulose-based native and surface modified fruit peels for the adsorption of heavy metal ions from aqueous solution: Langmuir adsorption isotherms, J. Chem. Eng. Data 55 (2009) 1186–1192.
[34] B.H. Hameed, A.A. Ahmad, Batch adsorption of methylene blue from aqueous solution by garlic peel, an agricultural waste biomass, J. Hazard. Mater. 164 (2009) 870–875.
[35] B.H. Hameed, D.K. Mahmoud, A.L. Ahmad, Equilibrium modeling and kinetic studies on the adsorption of basic dye by a low-cost adsorbent: Coconut (*Cocos nucifera*) bunch waste, J. Hazard. Mater. 158 (2008) 65–72.
[36] A.P. Vieira, S.A.A. Santana, C.W.B. Bezerra, H.A.S. Silva, J.A.P. Chaves, J.C.P. de Melo, E.C. da Silva Filho, C. Airoldi, Kinetics and thermodynamics of textile dye adsorption from aqueous solutions using babassu coconut mesocarp, J. Hazard. Mater. 166 (2009) 1272–1278.
[37] A.P. Vieira, S.A.A. Santana, C.W.B. Bezerra, H.A.S. Silva, J.A.P. Chaves, J.C.P. Melo, E.C. Filho, C. Airoldi, Removal of textile dyes from aqueous solution by babassu coconut epicarp (*Orbignya speciosa*), Chem. Eng. J. 173 (2011) 334–340.
[38] K. Amel, M.A. Hassen, D. Kerroum, Isotherm and kinetics study of biosorption of cationic dye onto banana peel, Energy Procedia 19 (2012) 286–295.
[39] Z. Zhang, L. Moghaddam, I.M. O'Hara, W.O.S. Doherty, Congo Red adsorption by ball-milled sugarcane bagasse, Chem. Eng. J. 178 (2011) 122–128.
[40] Z. Aksu, I.A. Isoglu, Use of agricultural waste sugar beet pulp for the removal of Gemazol turquoise blue-G reactive dye from aqueous solution, J. Hazard. Mater. 137 (2006) 418–430.
[41] M. Ertaş, B. Acemioğlu, M.H. Alma, M. Usta, Removal of methylene blue from aqueous solution using cotton stalk, cotton waste and cotton dust, J. Hazard. Mater. 183 (2010) 421–427.
[42] A. Saeed, M. Sharif, M. Iqbal, Application potential of grapefruit peel as dye sorbent: Kinetics, equilibrium and mechanism of crystal violet adsorption, J. Hazard. Mater. 179 (2010) 564–572.
[43] S.J. Allen, G. McKay, K.Y.H. Khader, Intraparticle diffusion of a basic dye during adsorption onto sphagnum peat, Environ. Pollut. 56 (1989) 39–50.
[44] N. Dizge, C. Aydiner, E. Demirbas, M. Kobya, S. Kara, Adsorption of reactive dyes from aqueous solutions by fly ash: Kinetic and equilibrium studies, J. Hazard. Mater. 150 (2008) 737–746.
[45] Z. Zhang, I.M. O'Hara, G.A. Kent, W.O.S. Doherty, Comparative study on adsorption of two cationic dyes by milled sugarcane bagasse, Ind. Crops Prod. 42 (2013) 41–49.
[46] C.C.A. Leal, O.R.S. Rocha, M.M.M.B. Duarte, R.F. Dantas, M. Motta, N.M. Lima Filho, V.L. da Silva, Evaluation of the adsorption process of remazol black b dye in liquid effluents by green coconut mesocarp, Afinidad 67 (2010) 136–142.
[47] G. Annadurai, R.-S. Juang, D.-J. Lee, Use of cellulose-based wastes for adsorption of dyes from aqueous solutions, J. Hazard. Mater. 92 (2002) 263–274.
[48] C. Namasivayam, D. Prabha, M. Kumutha, Removal of direct red and acid brilliant blue by adsorption on to banana pith, Bioresour. Technol. 64 (1998) 77–79.